Energetic evaluation of a double-effect LiBr-H_2O absorption heat pump coupled to a multi-effect distillation plant at nominal and off-design conditions

Aicha Chorak[1,2], Patricia Palenzuela[3*], Diego-César Alarcón-Padilla[3], Abdellatif Ben Abdellah[1,2]

[1]Abdelmalek Essaâdi University, Faculty of Science and Technology of Tangier, Research Team in Engineering, Innovation, and Management of Industrial Systems, Ziaten. BP: 416, Tangier, Morocco
[2]International University of Rabat, Renewable Energy, and Advanced Materials laboratory (REAM), Technopolis Rabat-Shore Rocade, Sale, Morocco
[3]CIEMAT-Plataforma Solar de Almería, Ctra. de Senés s/n, 04200 Tabernas, Almería, Spain
*Corresponding author. E-mail address: patricia.palenzuela@psa.es (P. Palenzuela),
E-mail addresses: chorakaicha@gmail.com, diego.alarcon@psa.es, benabdellah.abdellatif@gmail.com

Abstract

This paper presents the experimental characterization of a double-effect absorption heat pump (DEAHP) using lithium bromide-water (LiBr-H_2O) which recovers the low-energy latent heat from the last effect of a multi-effect distillation (MED) plant. The experimental facility is located at the Plataforma Solar de Almería (PSA) and the test campaign has been performed with the aim to find the best operating strategies that minimize the energy consumption and maximize the energetic efficiency of the DEAHP-MED system taking also into account the distillate production of the MED unit. For this purpose, the impact of the variation of the input variables by which the DEAHP-MED system can be controlled (MED inlet hot water flow rate, MED inlet hot water temperature, the live steam flow rate and the DEAHP cooling water flow rate) on the coefficient of performance (COP), the performance ratio (PR) and on the total distillate production, has been analysed in two different coupling schemes between the DEAHP and the MED unit (indirect and direct). The results revealed that in direct mode, the rise in the live steam flow rate has the greatest impact on the distillate production and the increase of the MED inlet hot water flow rate and the DEAHP cooling flow rate on the COP. In the indirect mode, the rise in the MED inlet hot water temperature was the most influential in both parameters. The maximum COP, distillate production and PR was 2.08±0.34, 2.42±0.07 m^3/h, and 18.53±1.94, respectively in the direct mode and 2.04±0.39, 1.92±0.11 m^3/h, 16.67±3.42, respectively the indirect mode. Moreover, empirical correlations that forecast the PR and the distillate production as a function of the COP were developed from the characterization results and were validated statistically by the coefficient of determination (R^2) and the adjusted R^2(R^2_{adj}).

***Keywords*:** Thermal desalination; Absorption heat pump; Multi-effect distillation; Energetic efficiency; Experimental characterization; Empirical equations

1. Introduction

One of the best options to make an MED process competitive with respect to reverse osmosis is to increase its energy efficiency. There are different possibilities but the most efficient one is recovering part of the thermal energy rejected in the distillation process with a heat pump, Adsorption Heat Pump (ADHP) or Absorption Heat Pump (AHP). The recovery and thus the energy efficiency of the system are higher when the AHP has two generators (double-effect absorption heat pump, DEAHP), so it is of great interest to couple MED units with DEAHPs.

On one hand, the coupling of an MED unit with an ADHP was investigated from theoretical and experimental points of views at the King Abdullah University of Science and Technology. Thu *et al.* [1-4] proved by simulation that the water production rate of the ADHP-MED system is considerably raised (up to twice) in comparison with a conventional MED for a hot water inlet temperature of 75 °C while the performance ratio (PR, defined as the mass in kg of distillate produced by the thermal energy supplied to the process normalized to 2326 kJ (1000 Btu) that is the latent heat of vaporization at 73 °C [5]) and the gain output ratio, GOR (defined as the mass ratio between the distillate production and the thermal energy consumed by the system [6]) were improved by 40%. Latter, Shahzad *et al.* [7-9] demonstrated experimentally the excellent thermodynamic synergy of the ADHP-MED system and proved that the water production increased up to 2.5 to 3 times in comparison with a conventional MED, which was in good agreement with their theoretical simulation. Also, it was found that PR of MED system was increased with the raise of the heat source temperature.

On the other hand, the use of AHPs to increase and improve the efficiency of MED plants was also evaluated experimentally and theoretically by several researchers. Ziqian [10, 11] *et al.* performed an experimental study of a solar AHP coupled to a Low-Temperature MED desalination system with four effects to evaluate the freshwater production and the COP (defined as the heat transfer rate delivered by the absorber and condenser of the DEAHP divided by the heat transfer rate from the gas boiler consumed by the DEAHP [12]) at different temperatures and pressures. The authors proved that higher COP were obtained at higher operating temperatures and lower seawater flow rates and that the freshwater production increased linearly with the rise in the operating temperatures. Alarcón-Padilla *et al.* [13] evaluated the operation of a DEAHP-MED system driven by a propane gas boiler. From the results, it was found a $COP$of 2 and a PR of 20, the double compared to the MED without the DEAHP. Palenzuela *et al.* [12] identified experimentally the challenges of a DEAHP-MED system from a control point of view. New operating strategies were proposed to increase the energetic efficiency of the system, being the main one a new control system implemented that resulted in an increase of the COP of 4%. Recently, Stuber *et al.* [14] performed an experimental and simulation study of an MED unit operating with and without an AHP, in order to reduce the process overall energy requirement. It was found that, when the experimental system was operated in "MED-only mode", the maximum PR obtained was 2.52, and the minimum specific energy consumption, (SC, defined as the ratio between energy input in kWh and total water produced in m^3) about 261.87 kWh_{th}/m^3, while operating in "AHP–MED mode", the maximum PR was doubled (5.27) and the minimum SC reached was 133.2 kWh_{th}/m^3. Furthermore, such authors carried out a simulation of a DEAHP–MED system, from which they obtained a substantial improvement in the PR and SC (18.4 and an SC of 34.9 kWh_{th}/m^3, respectively). Other authors have investigated the effect of certain parameters on the COP and the water production of the system. Wang and Lior [15] performed a simulation of a single effect LiBr-H_2O AHP-MED unit to study the influence of different factors on the thermodynamic performance of the whole system. The results showed that the higher motive steam pressure and generator approach temperature (which is the difference between the saturated temperature of the motive steam and that one of the strong solution at the exit of the generator) the higher the improvement in the water production for the same energy input and the higher the improvement in energy-efficiency of the AHP-MED system. Also, the results showed that increasing the strong-and-weak solution concentration difference, ΔX, the COP of the AHP-MED system is improved, reaching a maximum COP of

roughly 1.015. Li *et al.* [16] evaluated the performance of an AHP-MED unit with compression by a steady-state thermodynamic model. The results showed that the COP was increased raising the generator pressure and lowering the absorber pressure. Wang and Lior [17, 18] investigated the performance of a combined system composed of a single-effect LiBr–H_2O absorption refrigeration heat pump (ARHP) and a 6-effect MED unit by a mathematical model and a parametric sensitivity analysis. The authors showed that higher generator approach temperatures (9–13 ºC) and higher concentration differences between the strong and the weak solution (from 3% to 6%) lead to an increase in the water production of the MED plant by 6%. Ammar *et al.* [19] performed a techno-economic feasibility study in terms of COP for two systems: (i) AHP-MED system and (ii) Humidification-Dehumification (HD). The authors showed that the maximum COP for the AHP-MED system was found at an absorption pressure of 6, 6.5, and7.25 bar and their corresponding temperatures (64, 67, and 70 °C, respectively) and at a temperature in the generator of 52 °C. Moreover, it was proved that the distillate production of the AHP-MED system was two to three times larger than the one obtained with the HD process. Esfahani *et al.* [20] conducted an advanced exergy and exergoeconomic analysis to determine the most influential components on the overall system performance of an AHP-MED system compared with a MED unit using thermal vapor compression (TVC). The simulation results showed that the AHP-MED system was the best one resulting in an improvement in the exergy efficiency of 6.47% and of 5% in the GOR in comparison with the MED-TVC system. Srinivas *et al.*[21] developed a simulation model to determine the performance of an integrated Absorption Heat Transformer (AHT)with an MED unit of 14 effects for several working fluid combinations and at different operating conditions with the aim to maximizing the COP, PR and distilled water flow. Results showed that the COP decreases when the gross temperature lift (GTL), defined as the temperature differential between the absorber temperature and the generator temperature, is raised from 10 °C to 40 °C. Also, it was found that the COP and the distillate production for all working fluid combinations increase when the heating source temperature rises from 60 °C to 80 °C. However, the distillate production showed a decrease with the increase in the condenser temperature from 10 °C to 40 °C, and the PR resulted to be the same for all working fluid combinations. Sekar *et al*. [22] carried out an energy and exergy analysis of an AHT-MED system with a MED plant of three effects in order to evaluate the effect of various variables on the COP and on the exergy efficiency of the system. On one hand, the authors found that the COP increased from 0.444 to 0.498 with a variation in the GTL from 10 °C to 30 °C. On the other hand, it was found that the COP of the system raised with the increase of the solution heat exchanger effectiveness and of the temperature of the generator. Recently, Hamidi *et al.* [23] performed a comprehensive thermodynamic analysis and an efficiency assessment of two systems: Open absorption heat transformer (OAHT) integrated with a single effect distillation system and an OAHT integrated with an MED unit. A parametric study was carried out to evaluate the impact of three parameters on the $COP$and on the water production. The authors showed that, for the MED configuration, the COP was raised with higher absorber temperatures and the distillate production was reduced, while for the OAHTs-single-effect distillation system, this parameters remained constant. In addition, it was found that the COP of the OAHT-MED system was decreased for higher feedwater temperatures and the distillate production was raised between 10 and 15%.

From the previous literature review, it is proved that very few works, especially experimental ones, are based on the coupling of MED with DEAHP, being this option the one that provides the highest energy efficiency of the desalination plant. Experimental studies are especially important since they can be very useful for model validations, establishment of the best control strategies and for decision-making analyses. The present paper presents an exhaustive experimental analysis of the operation of a fossil DEAHP using LiBr-H_2O coupled to a MED

plant (last effect heat recovery) to increase its efficiency, in two coupling modes: direct and indirect, both at nominal and partial load conditions. The experimental characterization aims to determine the optimum operating conditions and the best-operating strategies that minimize the energy consumption and maximize the energetic efficiency of the system taking also into account the distillate production of the MED plant. For this purpose, a total of 22 experiments have been performed and the influence of the input variables by which the system can be controlled (the MED inlet hot water flow rate (F_{hMED}), the MED inlet hot water temperature (T_{hinMED}), the live steam flow rate (F_{SB}) and the DEAHP cooling water flow rate (F_{CW})) on the COP, the $PR$and on the distillate production ($\dot{m}_d$) has been evaluated from an energetic point of view. In addition, empirical correlations that forecast the PR and the $\dot{m}_d$ as a function of the COP, have been developed and validated statistically.

2. Material and Methods

Figure 1 represents the general layout of how the components of the experimental facility are integrated. The DEAHP is driven by high-pressure steam (steam at 180 ºC, 10 bar a) generated in a propane gas boiler while it recovers the low-pressure steam (35 ºC, 0.056 bar a) from the MED last effect, providing hot water to the MED unit (66.5 ºC, 1 bar).

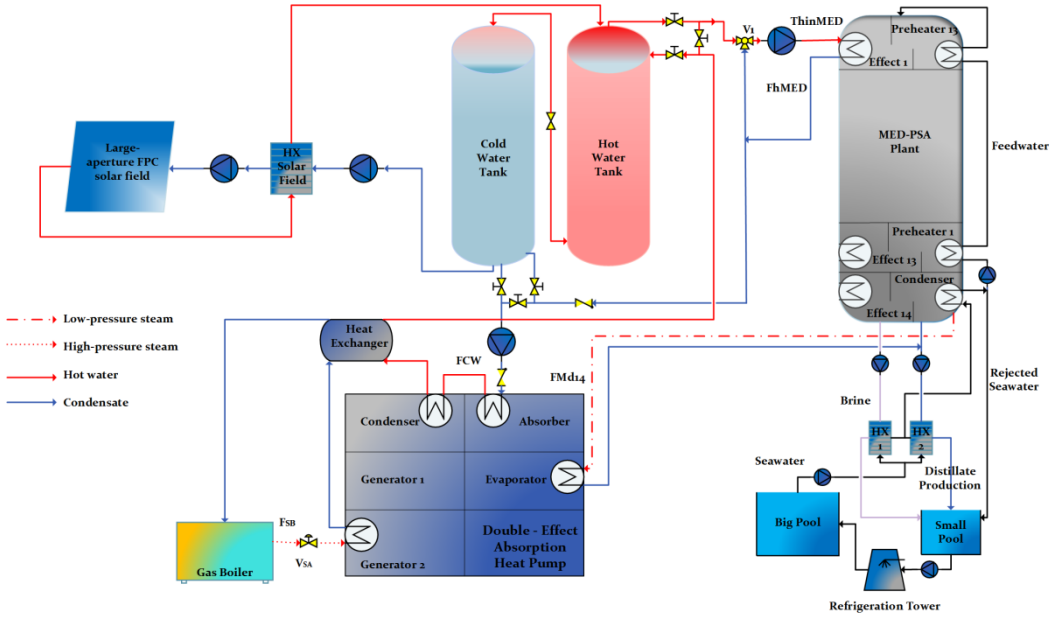

Figure 1. Layout of the DEAHP-MED desalination facility at the PSA

2.1 Double-effect absorption heat pump system

The LiBr–H_2O DEAHP (see Figure 2 on the left and the layout in Figure 3) was manufactured by ENTROPIE in 2006 and was coupled with the existing PSA MED unit. The DEAHP includes a high-temperature generator (Generator 2), a low-temperature generator (Generator 1), an evaporator, an absorber and a condenser. The LiBr–H_2O solution flows in a series configuration of a close circuit between Absorber, Generator 2, and Generator 1.A propane gas boiler performs as a high-temperature heat source, supplying saturated steam at

180 °C (10 bar) at nominal conditions to Generator 2. This steam is condensed inside the tube side, where a steam trap avoids its escape at the end. Once saturation conditions at ambient pressure are established, the steam trap evacuates sensible heat of condensate. This condensate crosses first a sensible heat exchanger (as shown in Figure 3) and then returns to the gas boiler, closing the cycle. Inside Generator 2, the first desorption occurs at high temperature, and the solution and steam circulate to Generator 1as the energy source by natural convection. Before the solution arrives at Generator 1, it circulates through a sensible heat exchanger (HX_1) where its temperature is reduced. Inside Generator 1, the second desorption occurs at a lower temperature caused by the latent heat liberated at the steam condensation that arrives from tube side of Generator 2. The condensate is accumulated at the bottom of the Generator 1 and once the condensate water valve (V_W) is opened, the pressure gradient rejects the condensate to the Condenser. The steam generated by Generator 1 and the one produced by flash at the Condenser, because of the higher temperature condensate arriving from Generator 1, are condensed in the Condenser. The latent heat of this condensation transfers its thermal energy to the cooling water circuit (F_{CW}). The condensed water from the Condenser circulates by HX_3, a sensible heat exchanger, before arriving at the Evaporator that is at a lower pressure and temperature. The feed steam in the Evaporator is saturated vapour coming from the last effect of the MED-PSA plant at a nominal temperature of 35 ºC (0.056 bar). In the Evaporator tube side, the steam is condensed releasing its latent heat and part of its sensible heat to the water that circulates on the shell side. Part of this water is evaporated and enters the Absorber when it is absorbed by the LiBr solution coming from both generators, transferring its latent heat to the cooling water circuit (F_{CW}). The LiBr solution from Generator 1 is pumped by Pump 1 through HX_2 where its temperature is reduced and sent back to the Absorber, closing the cycle. The cooling water circuit (F_{CW}) connects the DEAHP with the MED plant. This circuit is the medium-temperature energy source which is heated up by the DEAHP, as shown in Figure 3.

Figure 2. DEAHP LiBr-H_2O facility at the PSA on the left and the programmable logic controller on the right

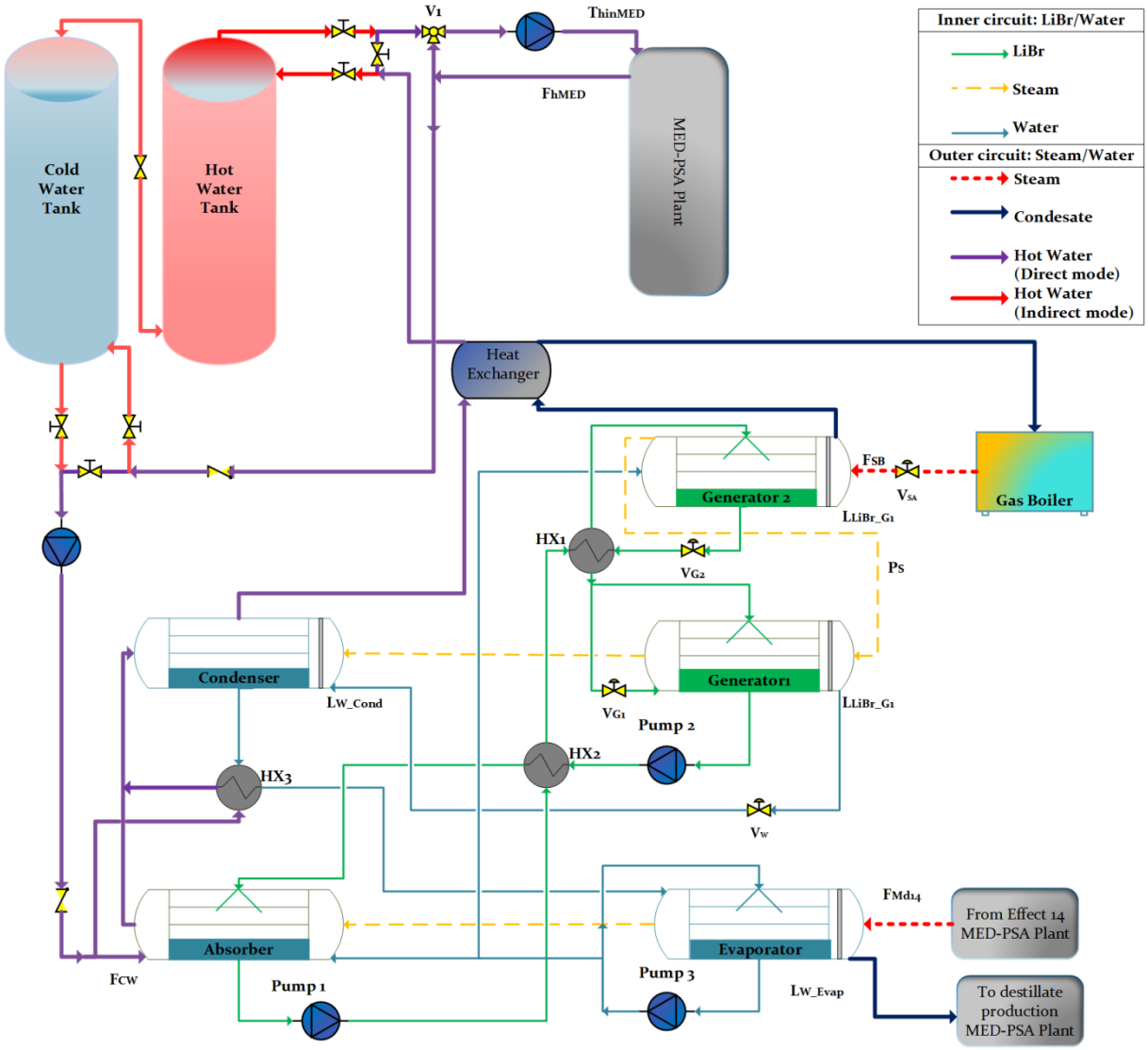

Figure 3. Schematic drawing of the two connections of the DEAHP to the MED unit

Table 1 shows the characteristics of all the components of the DEAHP-PSA.

Table 1

Type and characteristics of the DEAHP components

Heat exchangers	Type	Characteristics	Shell side	Tube side
Generator 1	Falling film	Fluid	LiBr	Steam
		Maximum pressure (bar)	0.5	5
		Maximum temperature (°C)	110	158
		Volume (L)	670	155
		Weight (kg)	586	
Generator 2	Submerged tubes	Fluid	LiBr	Steam
		Maximum pressure (bar)	5	13
		Maximum temperature (°C)	158	195
		Volume (L)	305	60.6
		Weight (kg)	476	
Evaporator	Falling	Fluid	Steam	Steam

	film	Maximum pressure (bar)	0.5	0.5
		Maximum temperature (°C)	110	60
		Volume (L)	960	88
		Weight (kg)	1615	
Absorber	Falling film	Fluid	Steam	H_2O
		Maximum pressure (bar)	0.5	6
		Maximum temperature (°C)	110	85
		Volume (L)	960	158
		Weight (kg)	1743	
Condenser	Falling film	Fluid	Steam	H_2O
		Maximum pressure (bar)	0.5	6
		Maximum temperature (°C)	110	85
		Volume (L)	670	90
		Weight (kg)	1611	

The DEAHP-PSA is equipped with monitoring instruments such as temperature and pressure sensors and flow meters that collect the experimental data every second and are displayed on a Human Machine Interface developed with LabVIEW of National Instruments. The temperatures are measured by means of Pt100 TR10-C class A in all cases. Smart pressure transmitters Cerabar PMC41 are used to measure the steam pressure from the Evaporator, the high-temperature Generator 2 and the low-temperature Generator 1. To quantify the volume of LiBr solution inside the Generators, the DEAHP has KRS magnetic level sensors. Flow rates are monitored using electromagnetic flow meters Endress+Hauser Proline Promag 50W forthe DEAHP cooling water flow rate,an ABB Vortex flow meter FV4000-VT4 for the flow rate of the saturated steam from the gas boiler (F_{SB}) and a paddle-wheel Bürkert S030 for the condensate mass flow rate coming from the last effect of the MED plant ($F_{\dot{M}_{d14}}$). Finally, there are two important regulation valves: steam valve (V_{SA}), which regulates the high-pressure steam flow rate from the gas boiler to Generator 2, and condensate water valve (V_W), which regulates the condensate flow rate between Generator 1 and Condenser. The first one has a pneumatic actuator Samson 3277 with electro-pneumatic positioner Samson 3730-2, and the second one has an electric actuator VALPES ER20.

Regarding the control system, a programmable logic controller (PLC) designed by ENTROPIE (see Figure 2 on the right) is available to start up the unit, to keep the operating parameters out of critical situations and to operate the DEAHP almost automatically (valve opening, LiBr and steam and water flow rates and pumps). More precisely, the PLC regulates the following elements:

- The steam flow rate from the boiler by V_{SA}.
- The condensate flow rate from the Generator 1 to the Condenser by V_W.
- The Generator 1 LiBr solution level (L_{LiBr_G1}),defined as the % of LiBr solution with respect to the generator chamber height in the Generator 1, by pump 1 (once the steady state is reached).
- Pump 1, Pump 2 and Pump 3: Pump 1 pumps the solution between the Absorber and Generator 2 and Pump 2 between Generator 1 and the Absorber. The Pump 3, situated at the bottom of the Evaporator, sucks water out and returns it back to the top of the Evaporator tube bundle.

The only parameter that is not controlled automatically is the Generator 2 LiBr solution level (L_{LiBr_G2}), which is defined as the percentage of LiBr solution with respect to the generator chamber height in the Generator 2. Its regulation (manually by V_{G2}) is very critical due to the importance of the DEAHP operation outside the crystallization zone.

2.2 Multi-effect Distillation Plant

The thermal desalination unit at the PSA is a forward-feed MED plant with 14 stages or effects, arranged vertically with the maximum pressure and temperature on the top. Further details can be found in [24]. Table 2 presents the specifications of the MED unit when is driven by the DEAHP at nominal conditions.

Table 2
Specifications of the MED unit driven by the DEAHP at nominal conditions

Parameters	Values
Power	150 kW_{th}
Inlet/outlet hot water temperature	66.5/63.5 °C
Brine temperature (on first cell)	62.0 °C
Cooling water flow rate	12.0 L/s
Hot water flow rate	12.0 L/s
Pressure drop	0.4 bar
Nominal plant production	2.7 m^3/h

2.3 Propane gas-fired boiler

The propane gas-fired tank (see Figure 4, on the left) was manufactured by Laguens y Pérez, S.L.U. The gas tank type LP2450A has an area of 10.1 m^2 and a volume of gas to be burnt of 2450 L. This volume provides an operational autonomy about 143 hours at full load.

Figure 4. The propane gas-fired tank (on the left) and the gas boiler (on the right)

The gas boiler type RL 200 (see Figure 4, on the right) was manufactured by ATTSU, and its characteristics and dimensions are shown in Table 3.

Table 3
Characteristics and dimension of the gas boiler

Parameters	Value
Maximum pressure (bar)	12.3
Maximum temperature (°C)	193
Total volume (L)	352
Water volume (L)	239
Thermal power (kW)	152
Empty weight (kg)	1100

2.4 DEAHP-MED system experimental characterization

The experimental characterization of the DEAHP-MED system has been performed with the aim to determine the optimum operating conditions and the best operating strategies that minimize the energy consumption and maximize the energetic efficiency of the system, taking also into account the distillate production. The characterization of the DEAHP-MED system was performed by assessing the impact of the variation of all the parameters that control the operation of the system on the distillate production, the COP and the PR. These two latter parameters are given by Eqs. (1) and (2):

$$COP = \frac{Q_{DEAHP}}{Q_{Boiler}} = \frac{Q_{Absorber} + Q_{Condenser}}{Q_{Boiler}} \quad (1)$$

$$PR = \frac{\dot{m}_d}{Q_{Boiler}} \cdot \frac{2326kJ}{1kg} \quad (2)$$

Two operation modes were evaluated depending on the coupling of the MED unit with the DEAHP: "indirect coupling", in which the DEAHP is coupled to the MED plant through the two water tanks (20 m^3 capacity each one) that are heated by a static solar field (see the corresponding circuit in Figure 3) and "direct coupling", in which the DEAHP is directly coupled to the MED plant, without the use of the water tanks (see the corresponding circuit in Figure 3). In the first operation mode, the temperature of the water entering the first effect of the MED plant is controlled by a three-way valve (V_1), and in the second one, the water achieves the temperature given by the operation of the DEAHP.

The experimental campaigns carried out in each operation mode are detailed below:

2.4.1 Indirect mode

- Case study 1: the live steam flow rate (F_{SB}) was varied from 24.63 m^3/h to 29.90 m^3/h. These flow rates correspond to the variation of the aperture of V_{SA}(AV_{SA}) from 40% to 50%. In this case, F_{hMED} and F_{CW} were kept constant at 12 L/s and T_{hinMED} at 65.8 °C.
- Case study 2: F_{CW} was varied between 7 L/s and 12 L/s. In these experiments, F_{hMED}, F_{SB} and T_{hinMED} were kept constant at 12 L/s, 39.14 m^3/h (corresponding to an AV_{SA} of 100%) and 61 °C, respectively.
- Case study 3: F_{CW} was varied between 7 L/s and 12 L/s. In these experiments, F_{hMED}, T_{hinMED} and F_{SB}were kept constant at 12 L/s, 66.4 °C and at 32.54 m^3/h (corresponding to an AV_{SA} of 100%), respectively.

- Case study 4: T_{hinMED} was varied between 60 °C and 66.5 °C. In these experiments, F_{hMED}, F_{CW}, and F_{SB} were fixed at 12 L/s, 12 L/s, and 26.65 m^3/h (corresponding to an AV_{SA} of 100%), respectively.

In all the cases, T_{hinMED} was kept constant at a certain value depending on the temperatures achieved in the storage tanks the previous day to the operation, which is in turn dependent on the solar radiation conditions.

2.4.2 Direct mode

- Case study 1: F_{SB} was varied from 23.35 m^3/h to 32.04 m^3/h. These flow rates correspond to the variation of the AV_{SA} from 40% to 50%. In this case, F_{hMED} was kept at 12 L/s and F_{CW} at 12 L/s.
- Case study 2: F_{CW} and F_{hMED} were varied between 7 L/s and 12 L/s. In these experiments, F_{SB} was kept fixed at 33.13 m^3/h (corresponding to an AV_{SA} of 100%).

An error analysis was performed considering the measurements uncertainty of all the instruments and the standard deviation (the highest value between both was chosen). The measurement uncertainties (U) of the measured variables of the DEAHP and MED plant are shown in Table 4.

The standard deviation (based on the entire population) is determined using the following formula:

$$\sqrt{\frac{\sum(x-\bar{x})^2}{n}} \tag{3}$$

where x is the sample mean average, $\bar{x}$ is the mean value of these observations and n is the sample size.

In the case of COP and PR (indirect parameters), an uncertainty propagation analysis was carried out in order to calculate how the uncertainties of the measured variables (boiler steam flow rate, inlet and outlet live steam temperature, cooling water flow rate, inlet and outlet temperature of the DEAHP condenser, inlet and outlet temperature of the DEAHP absorber and distillate production mass flow rate) propagate into these indirect variables. For this purpose, a tool of the Engineering Equation Solver (EES) software described in [25] was used.

The uncertainty propagation is calculated by the following equation:

$$U_Y = \sqrt{\sum_i \left(\frac{\partial Y}{\partial X_i}\right)^2 U_{X_i}^2} \tag{4}$$

where X_i is the vector of measured variables, Y the calculated variables (COP and PR) and U represents the uncertainty of the variable.

Table 4

Measurements uncertainty of the direct variables

Equipment	Variable	Instrument	Symbol	Measurement uncertainty
MED	Distillate water mass flow rate	Magnetic Flow meter, Model: D10D	$U_{\dot{m}_d}$[kg/s]	0.75% o.r.
DEAHP	Cooling water flow rate	Electromagnetic flow measurement, Model: Promag 50W	$U_{F_{CW}}$[m/s]	± 0.2% o.r.*
	Boiler steam flow rate	Vortex Flowmeter, Model: FV4000-VT4	$U_{F_{SB}}$[m^3/h]	± 1 % o.r.*
	Inlet and outlet steam temperature	Pt1000, Model: TR10-C, class A	$U_{T_{Steam}}$[°C]	0.15+ (0.002×T**)
	The inlet and outlet temperature of the condenser and absorber		$U_{T_{CW\_in}}$[°C] $U_{T_{CW\_out}}$[°C] $U_{T_{ABS\_in}}$[°C] $U_{T_{ABS\_out}}$[°C]	

*o.r. = of reading

**is the value of the temperature in °C

All the measurements were taken after steady state conditions were reached in the DEAHP-MED system and the average value of each parameter was determined. Water vapour thermophysical properties were calculated with XSteam Excel v2.6 according to IAPWS IF 97 [26, 27].

3. Experimental results and discussion

3.1 Experimental characterization of the DEAHP-MED system

3.1.1 Indirect mode

Case study 1: Influence of the live steam flow rate on the COP, PR and distillate production

Figure 5 shows the variation of COP, PR, and $\dot{m}_d$ for a F_{SB} range of 24.63 -29.90 m^3/h.

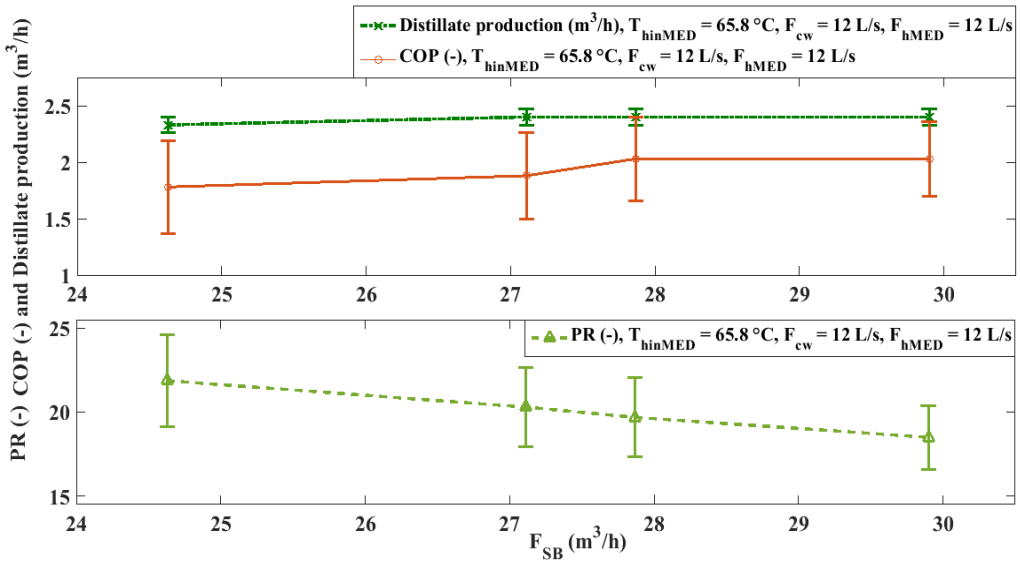

Figure 5. Results of $\boldsymbol{COP}$, distillate production, $\boldsymbol{PR}$ and their corresponding errors bars with the variation of $\boldsymbol{F_{SB}}$.

It can be seen that the distillate production ($\dot{m}_d$) rises with the F_{SB} from 24.63 m^3/h to 27.11 m^3/h since more motive steam flow rate is used to drive the DEAHP. The distillate production increases by a percentage of 3% but at expense of a rise in the DEAHP energy consumption (Q_{Boiler}) of 10.92%. Nevertheless, the $\dot{m}_d$ was kept constant in the range of F_{SB} from 27.11 m^3/h to 29.90 m^3/h. It was also observed an important rise in the COP (14.46%) when F_{SB} increased from 24.63 m^3/h to 27.87 m^3/h, since the increase in the heat transfer rate delivered by the DEAHP (31.15%)was higher than the increase in the heat transfer rate from the gas boiler to the DEAHP (14.31%). However, this parameter was kept constant in the range of F_{SB} from 27.87 m^3/h to 29.90 m^3/h. The trend found for the COP isin agreement with the work published in [28]. On the other hand, the PR decreased with a high percentage of 18.21% from 24.63 m^3/h to 29.90 m^3/h, which was due to the fact that distillate production was kept constant from 27.11 m^3/h to 29.90 m^3/h, and the Q_{Boiler} was raised (9.79%) in the same range.

From the results found in this study, if the operating strategy is to produce more distillate at maximum COP and higher efficiency, the optimum F_{SB}would be 27.87 m^3/h that leads to a PR of the MED unit of 19.69±2.35, a COP of the DEAHP of 2.03±0.37 and a distillate production of 2.40±0.07 m^3/h.

Case study 2: Influence of the water flow rate in the cooling circuit of the DEAHP on the COP, PR and distillate production

Figure 6 shows the variation of COP, PR and distillate production when F_{CW} varies between 7 and 12 L/s.

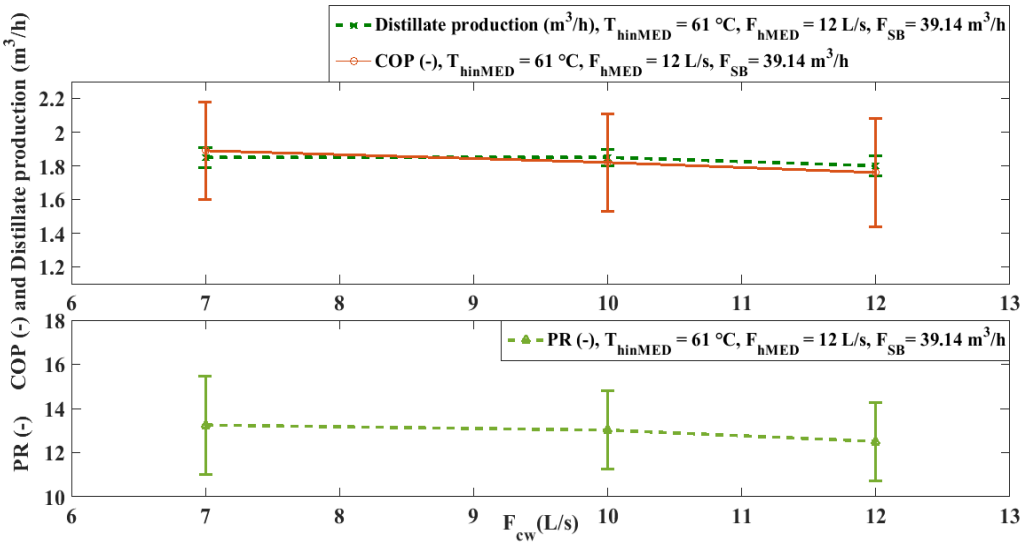

Figure 6. Results of $\boldsymbol{COP}$, distillate production and $\boldsymbol{PR}$ and their corresponding errors bars with the variation of the $\boldsymbol{F_{CW}}$.

It was observed that both, the distillate production and COP decreased with the increase of the F_{CW}. The former decreased with a percentage of 2.90% to reach a minimum of 1.80±0.06 m^3/h, and the latter with a percentage of 7.65%, resulting in a minimum of 1.76±0.32. The decrease in the COP is due to the increase of Q_{Boiler} (9.49%) and to the decrease of Q_{DEAHP} (2.41%). Accordingly, the optimum F_{CW}would be 7 L/s which gives the highest COP (1.89±0.29) and makes the MED unit producing the maximum amount of distillate (1.85±0.06 m^3/h) at its maximum efficiency (PR 13.25±2.22). Apart from that, lower values of F_{CW} would lead to a reduction in the electric consumption of the system, which also would favour its energetic optimization.

Case study 3: Influence of the inlet hot water flow rate of the MED plant on the COP, PR and distillate production

Figure 7 shows the variation of COP, PR, and distillate production when the F_{hMED}varies from 7 to 14 L/s.

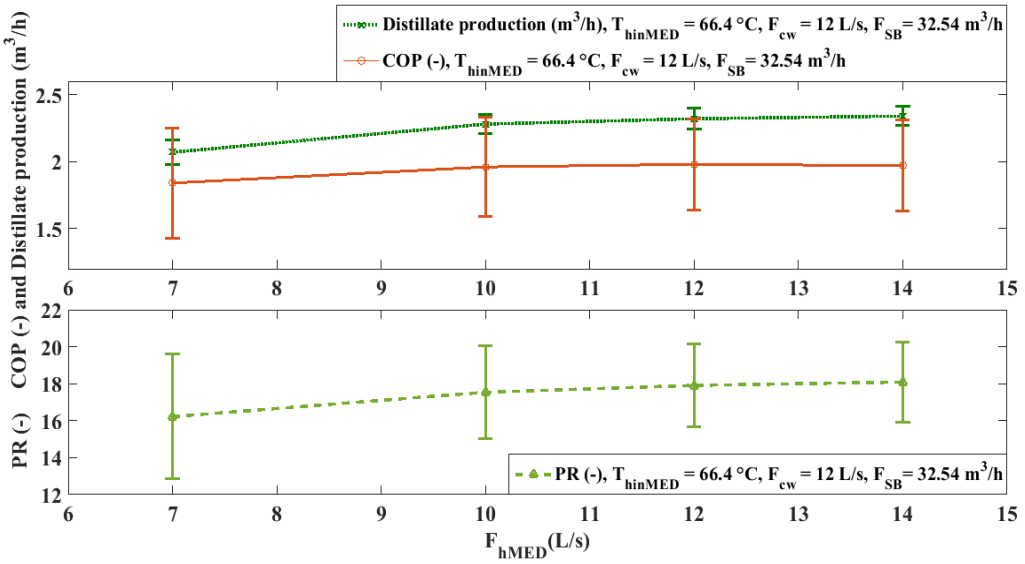

Figure 7. Results of the $\boldsymbol{COP}$, distillate production, the $\boldsymbol{PR}$ and their corresponding errors bars with the variation of $\boldsymbol{F_{hMED}}$.

As it can be observed, the distillate production, PR and COP increased with the rise in F_{hMED} from 7 L/s to 12 L/s (11.89% in the first case, 10.39% in the second case and 7.86% in the third case). The improvement in the distillate production is because of an increase in the rate of vapour formation inside the first effect falling film evaporator as a result of a higher thermal power provided to this effect. It conducts to an increase in the vapour produced in the rest of effects and correspondingly to a rise in the distillate produced by the MED plant [24, 28-31]. Hot water flow rates higher than 12 L/s do not further favour the COP, which start slightly to decrease (with a percentage of 0.66%). It is important to highlight that, despite the lower distillate production and COP obtained at lower F_{hMED}, the initial operation of the DEAHP-MED system at 7 L/s could be preferable to make the temperature of the cold tank to increase quickly (the lower the hot water flow rate the higher the hot water temperature leaving the MED plant and therefore the higher the temperature of the water flowing to the cold tank) and thus to achieve the steady state in the DEAHP faster (hotter temperature at the entrance of the absorber is reached). As the increase in the distillate production from 12 L/s to 14 L/s is very low (0.99 %) and due to the decrease of the COP in that range, the optimum F_{hMED} under steady-state operation would be 12 L/s that gives a maximum COP of 1.98±0.34, a distillate production of 2.32±0.08 m^3/h and a PR of 17.91±2.24.

Case study 4: Influence of the inlet hot water temperature of the MED plant on COP, PR and distillate production

Figure 8 shows the variation of $\boldsymbol{COP}$, the $\boldsymbol{PR}$ and the distillate production against the variation of $\boldsymbol{T_{hinMED}}$ between 60 and 66.5 °C.

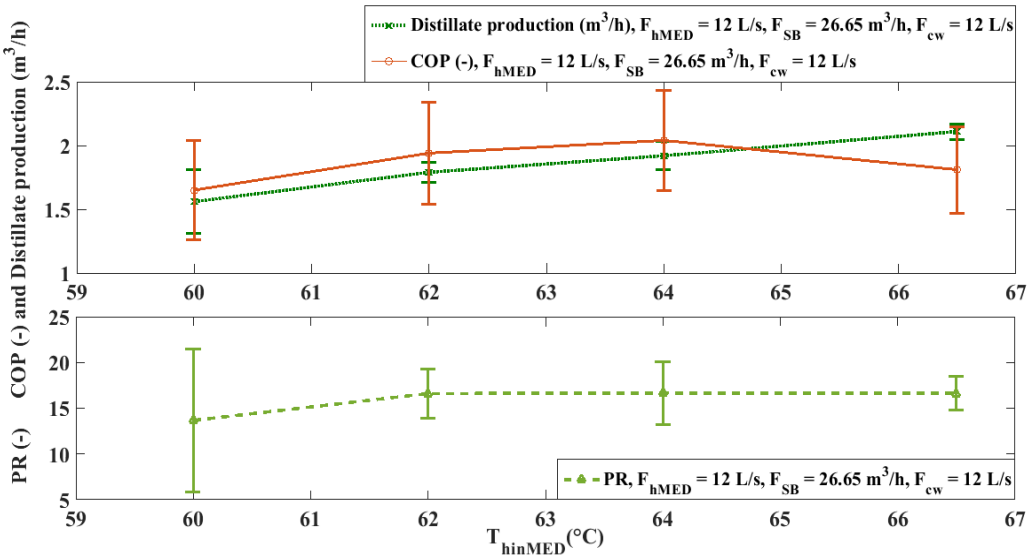

Figure 8. Results of $\boldsymbol{COP}$, distillate production, $\boldsymbol{PR}$ and their corresponding errors bars with the variation of $\boldsymbol{T_{hinMED}}$.

As it can be observed, the distillate production highly increased with the rise in T_{hinMED} from 60 °C to 66.5 °C (35.57%) reaching a maximum value of 2.11±0.06 m^3/h. These trends are in agreement with the work published in [19]. The great increase in the distillate production is due to the higher amount of vapour being produced in the MED first effect at higher

temperatures. These high temperatures lead to a higher heat transfer rate from the outlet MED first effect to the cold tank and therefore to the entrance of the absorber of the DEAHP, which in turn increase the absorption process and thus the heat released by the DEAHP to the MED (Q_{DEAHP} increases a 22.53%). Such increase is achieved without an important rise in the heat provided by the boiler (11.47%). It can be observed that the COP highly increased with the rise in T_{hinMED} from 60 °C to 64 °C (23.19%) reaching a maximum value of 2.04±0.39. This trendis in agreement with the work published in [19]. The decrease found in theCOP when the hot water temperature increased from 64 to 66.5 ºC (12.50%) is in consistency with the works published in [32-37]. Therefore, the optimum T_{hinMED}under steady-state operation would be 64 °C that gives a maximum COP of 2.04±0.39, a distillate production of 1.92±0.11 m^3/h and makes the MED unit achieving the maximum PR of 16.67±3.42.

From all the results showed above, it has been observed that, in the indirect operation mode, the rise in the hot water inlet temperature entering the MED first effect has more influence in $\dot{m}_d$ and COP than the increase in F_{SB}, F_{hMED}, and F_{CW}.

3.1.2 Direct mode

Case study 1: Influence of the live steam flow rate on COP, PR and distillate production

Figure 9 shows the variation of the COP, the PR and distillate production versus the variation in F_{SB} from 25.35 m^3/h to 32.04 m^3/h.

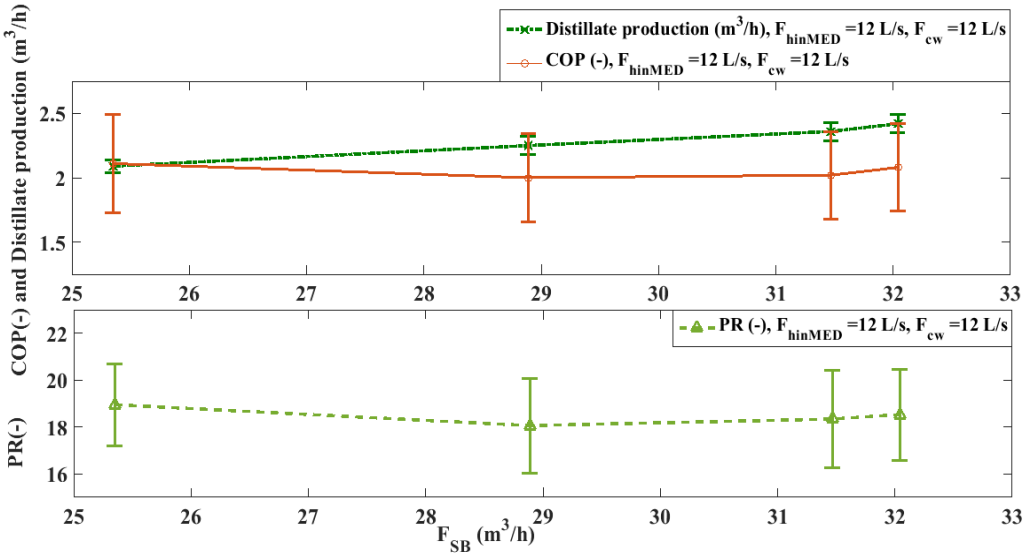

Figure 9. Results of the $\boldsymbol{COP}$, distillate production, the $\boldsymbol{PR}$ and their corresponding errors bars with the variation of $\boldsymbol{F_{SB}}$.

It is observed that the distillate production rises with the F_{SB} from 25.35 m^3/h to 32.04 m^3/h with a percentage of 15.68% to reach a maximum of 2.42±0.07 m^3/h. It is due to the fact that the heat transfer supplied from the DEAHP to the MED plant rises 8.84% with the increase in the F_{SB}, which promotes more evaporation in the MED unit and therefore more distillate production.

On the other hand, the COP reached the maximum value at a F_{SB} of 25 m^3/h (2.11±0.38). Then, it decreased with the F_{SB} (from 25.35 m^3/h to 28.89 m^3/h with a percentage of 5.10%, to

reach a minimum of 2.00, while the distillate production increased 7.88% in the same range. The COP gradually increased with the increase in the F_{SB} from 28.89 m^3/h to 32.04 m^3/h (with a percentage of 3.84%).These results are in consistency with the results obtained in Ref [13]. Likewise, the PR also achieved its maximum (18.95±1.75) at F_{SB} of 25 m^3/h. Hence, the optimum F_{SB} would be 32.04 m^3/h that give a high COP of 2.08±0.34, makes the MED unit produce the maximum distillate production of (2.42±0.07 m^3/h) and reach a high PR of 18.53±1.94

Case study 2: Influence of the water flow rate in the cooling circuit of the DEAHP and the inlet hot water flow rate of the MED plant on the COP, PR and distillate production

Figure 10shows the variation of the COP, the PR, and distillate production for F_{CW} and F_{hinMED} ranging from 7 to 12 L/s.

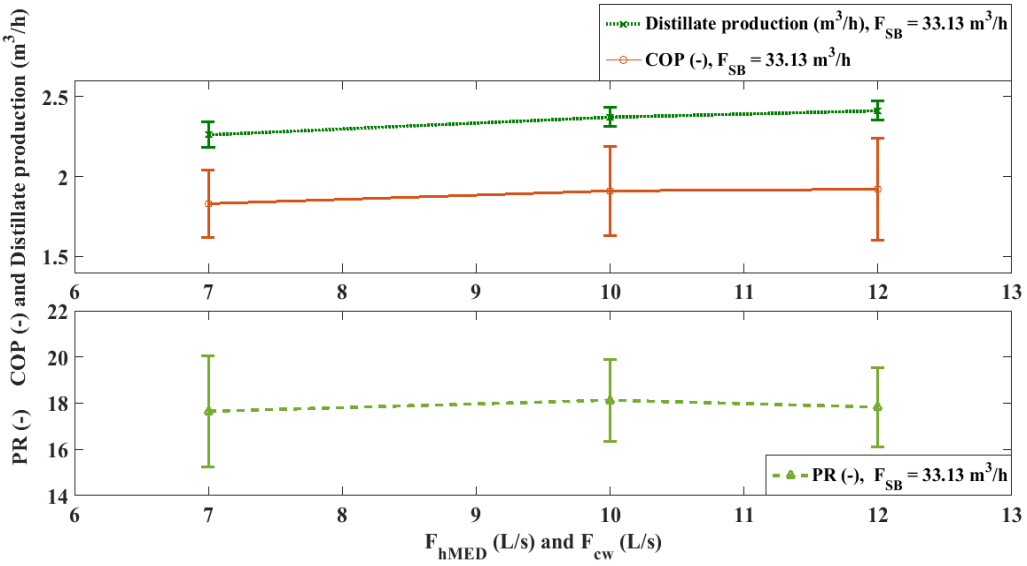

Figure 10. Results of $\boldsymbol{COP}$, distillate production, the $\boldsymbol{PR}$ and their corresponding errors bars with variation of $\boldsymbol{F_{hMED}}$ and $\boldsymbol{F_{CW}}$.

As it can be observed, the COP slightly increased with the rise of the F_{CW} and F_{hMED}between 7 L/s and 12 L/s (with a percentage of 4.93%), which match with the work stated in Refs [28, 38]. The significant increase in COP with F_{hMED} and F_{CW} can be because the increase of these two parameters helps to raise the heat transfer coefficients of the absorber and condenser falling films in the case of DEAHP and of the first effect falling film in the case of the MED plant, increasing the Q_{DEAHP}(10.90%). Likewise, as previously discussed, the increase in Q_{DEAHP} leads to a rise in the vapour formation inside the MED plant and therefore in the distillate production, achieving an increase of 6.78%. These results match with those ones found in the works published in [24, 29-31]. Concerning the PR, it can be observed that it increased (2.73%) from 7 to 10 L/s and then it started to decrease with a percentage of 1.68% from 10 L/s to 12 L/s. The maximum value was obtained at 10 L/s (18.89). This can be due to the increase in Q_{Boiler} of 2.11% from 7 to 10 L/s and of 3.35% from 10 to 12 L/s. Thus, the optimum F_{hMED} and F_{CW}would be 12 L/s that give a maximum COP of 1.92±0.32, a maximum amount of distillate production of 2.41±0.06 m^3/h and a PR of 17.83±1.72.

From all the previous results, it can be seen that the rise in F_{SB} has more influence in $\dot{m}_d$ than that of F_{hinMED} and F_{CW}. In the case of the COP, the rise of $F_{hMED}$and F_{CW} from 10 to 12 L/s at a F_{SB} of 33.13 m^3/h has more influence than the rise in the F_{SB}.

From all the prior results in indirect and direct mode, the optimum operation points have been selected (see Table 5) according to the objective to be accomplished: minimize the energy consumption and maximize the energy efficiency of the system taking also into account the distillate production.

Table 5

Optimum results of the operation of the DEAHP-MED system for different study cases

Operation mode	Study cases	F_{SB} (m^3/h)	F_{hMED} (L/s)	F_{CW} (L/s)	T_{hinMED} (°C)	PR	COP	$\dot{m}_d$ (m^3/h)
Indirect mode	Case 1	27.87	12.00	12.00	65.78	19.69±2.35	2.03±0.37	2.40±0.07
	Case 2	39.14	12.00	7.00	61.01	13.25±2.22	1.89±0.29	1.85±0.06
	Case 3	32.54	12.00	12.00	66.54	17.91±2.24	1.98±0.34	2.32±0.08
	Case 4	26.65	12.00	12.00	64.01	16.67±3.42	2.04±0.39	1.92±0.11
Direct mode	Case 1	32.04	12.00	12.00	70.24	18.53±1.94	2.08±0.34	2.42±0.07
	Case 2	33.13	11.97	12.00	65.83	17.83±1.72	1.92±0.32	2.41±0.06

Comparing the results in indirect and direct mode at the same cases and conditions, it can be noticed that: the case 1 in direct mode showed the best COP (2.08±0.34), a distillate production of 2.42±0.07m^3/h, and a PR of 18.53±1.94 at a $F_{SB}$of 32.04 m^3/h and establishing F_{hMED} and F_{CW} at design conditions, compared with the case 1 in indirect mode. However, the case 4 in indirect mode exhibited the maximum COP (2.04±0.39) and a distillate production of 1.92±0.11m^3/h and a PR of 16.67±3.42 at 26.65 m^3/h of F_{SB} and keeping F_{hMED} and F_{CW} at design conditions, compared with the case 2 in direct mode.

From the optimum results shown in Table 5, the best operating strategies that lead to the minimum energy consumption and the maximum energetic efficiency of the system have been selected. They are summarized in Table 6.

Table 6

The best selected optimum operating strategies of DEAHP-MED system

Operation mode	F_{SB} (m^3/h)	F_{hMED} and F_{CW} (L/s)	T_{hinMED} (°C)	Q_{Boiler} (kW)	PR	COP	$\dot{m}_c$ (m^3/h)
Indirect Mode	26.65	12.00	64.01	74.59	16.67±3.42	2.04±0.39	1.92±0.11
Direct Mode	32.04	12.00	70.24	84.39	18.53±1.94	2.08±0.34	2.42±0.07

As can be observed, the thermal power required by the boiler to accomplish the best operating strategies of the DEAHP-MED system is 74.59 kW_{th} in the case of indirect mode, and 84.39 kW_{th} in the case of direct mode.

3.1.3 Empirical correlations

The following empirical correlations have been obtained from the results from the experimental characterization.

The empirical correlation between the PR and the $COP$is expressed by the following equation:

$$PR = (-15.56 \cdot COP^2) + (69.61 \cdot COP) - 58.81 \quad (5)$$

The correlation is valid for the following range of COP:

$$1.50 \leq COP \leq 2.20$$

The empirical correlation between the $\dot{m}_d$ and the COP is expressed by the following equation:

$$\dot{m}_d = (-7.531 \cdot COP^2) + (29.66 \cdot COP) - 26.91 \quad (6)$$

The equation is accurate for the following range of COP:

$$1.6 \leq COP \leq 2.3$$

The two correlations developed have been validated statistically by calculating the dimensionless coefficient of determination (R^2) and the adjusted R^2(R^2_{adj}). The statistical results that prove the goodness of the parametric correlations are shown in Table 7. As can be observed, the relatively high values of $0.95<R^2<0.97$ and $0.94<R^2_{adj}<0.97$ reveal that all the empirical correlations determined are great candidates to represent the behaviour of the PR and $\dot{m}_d$ in the DEAHP-MED system.

Table 7
The statistical results for the evaluation the goodness of fit

Statistical parameters	Eq. (5)	Eq. (6)
R^2	0.97	0.95
R^2_{adj}	0.97	0.94

4. Conclusions

In order to study the optimum operating points that minimize the energy consumption and maximize the energy efficiency of the DEAHP-MED system, the influence of various key parameters that control the operation of the system on its performance has been investigated by an experimental characterization at different operation modes. The results of the COP,

distillate production and PR in the different cases has been presented and analysed. Some conclusions driven from this experimental analysis are drawn as follows:

(1) In the indirect mode, the COP and distillate production increase with the raise of the live steam flow rate while the PR decreases. In addition, the COP, PR and distillate production increase with the raise of F_{hMED} and T_{hinMED}. However, these parameters decrease with the raise of F_{CW}. It results beneficial since lower values of F_{CW} would lead to a reduction in the electric consumption of the system, promoting its energetic optimization. The optimum operating conditions of the DEAHP-MED system are F_{SB} of 27.87 m^3/h, F_{CW} of 7 L/s, $F_{hMED}$of 12 L/s, and $T_{hinMED}$of 64 ºC, which lead to achieve a maximum COP of 2.04±0.39,a maximum PR and a maximum distillate production.
(2) In the direct mode, the COP, $PR$and distillate production increase with the raise of the live steam flow rate, F_{hMED} and F_{CW}. The optimum operating conditions of the DEAHP-MED system are F_{SB} of 32.04 m^3/h, F_{CW} and F_{hMED} of 12 L/sand T_{hinMED} of 70 ºC, leading to a maximum COP of 2.08±0.34, a higher PR, and a maximum distillate production.
(3) Comparing these optimum points with respect those ones obtained in the study of the MED unit operating without the DEAHP [24] but with solar energy, it is found that the distillate production obtained is similar but the PR with the DEAHP-MED system is nearly doubled.
(4) The operational parameters $F_{SB,}$ F_{hMED} and F_{CW} are the three main ones in the optimization of the DEAHP-MED unit operation in direct mode, while$T_{hinMED}$is the one in the indirect mode.
(5) The relative differences acquired can be extrapolated for other AHP-MED plants and the two empirical correlations presented of the PR and distillate production as a function of the COP can be useful for designers and researchers of AHP-MED systems for decision-making analyses.

Acknowledgments

The authors acknowledge funding support from the Spanish Ministry of Economy and Competitiveness and ERDF funds under the National R+D+I Plan Project DPI2014-56364-C2-2-R of the Spanish Ministry of Economy and Competitiveness and ERDF funds and the 7th Framework Programme of the EU (SFERA 2 Grant Agreement no. 312643). Likewise, the authors would like to extend their special thanks to ‘‘IRESEN” for bringing financial support to perform this research through the project ‘‘Seawater desalination using solar energy”, InnoTherm II Solar thermal applications and solar technologies support.

Nomenclature

Variables

F_{SB}	Live steam flow rate (m^3/h)
F_{CW}	DEAHP cooling water flow rate (L/s)
F_{hMED}	MED inlet hot water flow rate (L/s)
$F_{\dot{m}d14}$	Condensate mass flow rate coming from the last effect of the MED plant (m^3/h)
$\dot{m}_d$	Distillate production mass flow rate (m^3/h)
$Q_{Absorber}$	Thermal energy provided by the absorber of the DEAHP (kW)

Q_{Boiler}	DEAHP Gas boiler consumption (kW)
$Q_{Condenser}$	Thermal energy provided by the condenser of the DEAHP (kW)
Q_{DEAHP}	Thermal energy provided by the DEAHP (kW)
T_{ABS_in}	Absorber inlet temperature of the DEAHP (°C)
T_{ABS_out}	Absorber outlet temperature of the DEAHP (°C)
T_{CW_in}	Condenser inlet temperature of the DEAHP (°C)
T_{CW_out}	Condenser outlet temperature of the DEAHP (°C)
T_{hinMED}	MED inlet hot water temperature (°C)
T_{Steam}	Steam temperature of the DEAHP (°C)
U	Measurement uncertainties (–)
AV_{SA}	Boiler steam valve aperture (%)

559

560 ***Acronyms and abbreviations***

561

AHP	Absorption heat pump
COP	Coefficient of performance
DEAHP	Double effect adsorption heat pump
$LiBr-H_2O$	Lithium bromide-water
MED	Multiple effect distillation
PR	Performance ratio
PSA	Plataforma Solar de Almeria
REAM	Renewable Energy and Advanced Materials laboratory
SC	Specific energy
TES	Thermal energy storage

562

563 **References**

564 [1] K. Thu, Y.-D. Kim, G. Amy, W.G. Chun, K.C. Ng, A hybrid multi-effect distillation and adsorption
565 cycle, Applied Energy 104 (2013) 810–821. http://dx.doi.org/10.1016/j.apenergy.2012.12.007.
566 [2] K. Thu, Y.-D. Kim, G. Amy, W. G. Chun, K.C. Ng, A synergetic hybridization of adsorption cycle with
567 the multi-effect distillation (MED), Applied Thermal Engineering 62 (2014) 245–
568 255.http://dx.doi.org/10.1016/j.applthermaleng.2013.09.023.
569 [3] K. Thu, Y.-D. Kimb, M. Wakil Shahzad, J. Saththasivamd, K. C. Ng , Performance investigation of an
570 advanced multi-effect adsorption desalination (MEAD) cycle, Applied Energy 159 (2015) 469–
571 477.http://dx.doi.org/10.1016/j.apenergy.2015.09.035.
572 [4] M.W. Shahzad,K. C. Ng, K. Thu, B. B. Saha, W. G. Chun, Multi effect desalination and adsorption
573 desalination (MEDAD): A hybrid desalination method, Applied Thermal Engineering 72 (2014) 289-
574 297. https://doi.org/10.1016/j.applthermaleng.2014.03.064.
575 [5] P. Palenzuela, D. Alarcón, G. Zaragoza, Concentrating, Solar Power and Desalination Plants:
576 Engineering and Economics of Coupling Multi-Effect Distillation and Solar Plants, Springer
577 International Publishing, Switzerland, 2015. https://doi.org/10.1007/978-3-319-20535-9.
578 [6] P. Palenzuela, G. Zaragoza, D. Alarcón, Characterization of the coupling of multi-effect distillation
579 plants to concentrating solar power plants, Energy 82 (2015) 986–995.
580 http:/dx.doi.org/10.1016/j.energy.2015.01.109.

[7] M.W. Shahzad, K. Thu,Y.-d. Kimc, K. C. Ng, An experimental investigation on MEDAD hybrid desalination cycle, Applied Energy 148 (2015) 273–281. http://dx.doi.org/10.1016/j.apenergy.2015.03.062.
[8] M. W. Shahzad, K. Thu, K. Ch. Ng, C. WonGee, Recent development in thermally activated desalination methods: achieving an energy efficiency less than 2.5 kWhelec/m^3, Desalination and Water Treatment 57 (2015) 7396-7405. http://dx.doi.org/10.1080/19443994.2015.1035499.
[9] K. C. Ng, K. Thu, S.J. Oh, L. Ang, M.W. Shahzad, A. Bin Ismail, Recent developments in thermally-driven seawater desalination: energy efficiency improvement by hybridization of the MED and AD cycles, Desalination 356 (2015) 255–270. http://dx.doi.org/10.1016/j.desal.2014.10.025.
[10] C. Ziqiana, Z. Hongfeia, M. Chaochen,L. Zhengliang, H. Kaiyan, Experiment and optimal parameters of a solar heating system study on an absorption solar desalination unit, Desalination Water Treatment 1 (2009) 128-138. https://doi.org/10.5004/dwt.2009.106.
[11] Z. Hongfei, Solar Energy Desalination Technology, Chapter 8 – Absorption and Adsorption Solar Desalination System, first ed., Elsevier, 2017,623–670.https://doi.org/10.1016/B978-0-12-805411-6.00008-7.
[12] P. Palenzuela, L. Roca, G. Zaragoza, D. Alarcón-Padilla, L. García, A. de la Calle, Operational improvements to increase the efficiency of an absorption heat pump connected to a multi-effect distillation unit, Applied Thermal Engineering 63 (2014) 84–96. https://doi.org/10.1016/j.applthermaleng.2013.10.050.
[13] D. C. Alarcón-Padilla, L. García-Rodriguez, J. Blanco-Gálvez, Experimental assessment of connection of an absorption heat pump to a multi-effect distillation unit, Desalination 250 (2) (2010) 500–505. https://doi.org/ 10.1016/j.desal.2009.06.056.
[14] M. D. Stuber, C. Sullivan, S.A. Kirk, J.A. Farrand, P.V. Schillaci, B.D. Fojtasek, A.H. Mandell, Pilot demonstration of concentrated solar-powered desalination of subsurface agricultural drainage water and other brackish groundwater sources, Desalination 355 (2015) 186–196. https://doi.org/ 10.1016/j.desal.2014.10.037.
[15] Y. Wang, N. Lior, Thermoeconomic analysis of a low-temperature multi-effect thermal desalination system coupled with an absorption heat pump, Energy 36 (2011) 3878 – 3887. https://doi.org/ 10.1016/j.energy.2010.09.028.
[16] H. Li, N. Russell, V. Sharifi, J. Swithenbank, Techno-economic feasibility of absorption heat pumps using wastewater as the heating source for desalination, Desalination 281 (2011) 118–127. https://doi.org/ 10.1016/j.desal.2011.07.049.
[17] Y. Wang, N. Lior, Combined Desalination and Refrigeration Systems Driven by Low-Grade Heat, ASME proceedings:Energy Systems: Analysis, Thermodynamics and Sustainability; Sustainable Products and Processes, 8 (2008) 163-173. https://doi.org/ 10.1115/IMECE2008-67029.
[18] Y. Wang, N. Lior, Proposal and analysis of a high-efficiency combined desalination and refrigeration system based on the LiBr-H_2O absorption cycled part 1: system configuration and mathematical model, Energy Conversion and Management 52 (2011) 220-227.
[19] Y. Ammar, H. Li, C. Walsh, P. Thornley, V. Sharifi, A. P. Roskilly, Reprint of "Desalination using low grade heat in the process industry: Challenges and perspectives", Applied Thermal Engineering 53 (2013) 234-245. http://dx.doi.org/10.1016/j.applthermaleng.2012.05.012.
[20] I. J. Esfahani, S. Lee, C. Yoo, Evaluation and optimization of a multi-effect evaporation–absorption heat pump desalination based conventional and advanced exergy and exergoeconomic analyses, Desalination 359 (2015) 92–107. https://doi.org/ 10.1016/j.desal.2014.12.030.
[21] G. Srinivas, S. Sekar, R. Saravanan, S. Renganarayanan, Studies on a water-based absorption heat transformer for desalination using MED, Desalination and Water Treatment 1 (2009) 75–81.http://dx.doi.org/10.5004/dwt.2009.110.
[22] S. Sekar, and R. Saravanan, Exergetic performance of eco friendly absorption heat transformer for seawater desalination, International Journal of Exergy 8 (2011) 51–67. https://doi.org/10.1504/IJEX.2011.037214.
[23] A. Hamidi, K. Parhama, U. Atikol, A. H. Shahbaz, A parametric performance analysis of single and multi-effect distillation systems integrated with open-cycle absorption heat transformers, Desalination 371 (2015) 37–45. http://dx.doi.org/10.1016/j.desal.2015.06.003.

[24] A. Chorak, P. Palenzuela, D-C. Alarcón-Padilla, A.B. Abdellah, Experimental characterization of a multi-effect distillation system coupled to a flat plate solar collector field: empirical correlations, Applied Thermal Engineering 120 (2017) 298–313. https://doi.org/10.1016/j.applthermaleng.2017.03.115.
[25] G. Nellis, S. Klein, Heat Transfer, Cambridge University Press, New York, 2009.
[26] A. Saul, W. Wagner, International equations for the saturation properties of ordinary water substance, J. Phys. Chem. Ref. Data, 16 (4) (1987) 893–901.https://doi.org/ 10.1063/1.555787.
[27] W. Wagner, A. Pruss, International equations for the saturation properties of ordinary water substance.Revised according to the international temperature scale of 1990, J. Phys. Chem. Ref. Data 22 (3) (1993) 783–787.https://doi.org/ 10.1063/1.555926.
[28] B. Bakhtiari, L. Fradette, R. Legros, J. Paris, A model for analysis and design of H_2O–LiBr absorption heat pumps, Energy Conversion and Management 52 (2011) 1439–1448. https://doi.org/10.1016/j.enconman.2010.09.037.
[29] L. Yang, S. Shen, H. Hu, Thermodynamic performance of a low temperature multi-effect distillation experimental unit with horizontal-tube falling film evaporation, Desalination and Water Treatment 33 (2011) 202–208, http://dx.doi.org/10.5004/dwt.2011.2514.
[30] M. El-Nashar, A.A. Qamhiyeh, Simulation of the steady-state operation of a multi-effect stack seawater distillation plant, Desalination 101 (1995) 231–243, http://dx.doi.org/10.1016/0011-9164(95)00026-X.
[31] J. Leblanc, J. Andrews, A. Akbarzadeh, Low-temperature solar-thermal multi-effect evaporation desalination systems, International Journal of Energy Research 34 (2010) 393–403, http://dx.doi.org/10.1002/er.1642.
[32] Md. Azhar, M. A. Siddiqui, Energy and Exergy Analyses for Optimization of the Operating Temperatures in Double Effect Absorption Cycle, Energy Procedia 109 (2017) 211–218. http://dx.doi.org/10.1016/j.egypro.2017.03.043.
[33] S. M. Tarique, M. A. Siddiqui, Performance and economic study of the combined absorption/compression heat pump, Energy Conversion and Management 40 (1999) 575–91. https://doi.org/10.1016/S0196-8904(98)00045-4.
[34] C. W. Park, J. Koo, Y.T. Kang, Performance analysis of ammonia absorption GAX cycle for combined cooling and hot water supply modes, International Journal of Refrigeration 31 (2008) 727–733.https://doi.org/10.1016/j.ijrefrig.2007.11.005.
[35] K. Parham, M. Khamooshi, S. Daneshvar, M. Assadi, M. Yari, Comparative assessment of different categories of absorption heat transformers in water desalination process, Desalination 396 (2016) 17–29. http://dx.doi.org/10.1016/j.desal.2016.05.031.
[36] R. Gomri, Thermal seawater desalination: Possibilities of using single effect and double effect absorption heat transformer systems, Desalination 253 (2010) 112–118.https://doi.org/10.1016/j.desal.2009.11.023.
[37] K. Parham, M. Yari, U. Atikol, Alternative absorption heat transformer configurations integrated with water desalination system, Desalination 328 (2013) 74–82.http://dx.doi.org/10.1016/j.desal.2013.08.013.
[38] M. Garrabrant, R. Stout, P. Glanville, C. Keinath, S.Garimella, Development of ammonia-water absorption heat pump water heater for residential and commercial applications, ASME 7th International Conference on Energy Sustainability, 2013.https://doi.org/10.1115/ES2013-18121.